

# Motion Planning for a Class of Planar Closed-Chain Manipulators

N. Shvalb, G. Liu<sup>†</sup>, M. Shoham, J.C. Trinkle<sup>‡</sup>

Dept of ME, Technion-Israel Institute of Technology, Israel, shvalbn@technix.technion.ac.il

<sup>†</sup> Dept of CS, Stanford University, liugf@cs.stanford.edu

<sup>‡</sup> Dept of CS, Rensselaer Polytechnic Institute, trink@cs.rpi.edu

**Abstract**— We study the motion planning problem for planar star-shaped manipulators. These manipulators are formed by joining  $k$  “legs” to a common point (like the thorax of an insect) and then fixing the “feet” to the ground. The result is a planar parallel manipulator with  $k - 1$  independent closed loops. A topological analysis is used to understand the global structure the configuration space so that planning problem can be solved exactly. The worst-case complexity of our algorithm is  $O(k^3 N^3)$ , where  $N$  is the maximum number of links in a leg. Examples illustrating our method are given.

## I. INTRODUCTION

The canonical robot motion planning problem is known as the “piano movers” problem. In this problem, one is given initial and goal configurations of a “piano” (a rigid body that is free to move in an environment with fixed rigid obstacles) and geometric models of the piano and obstacles. The goal is to find a continuous motion of the piano connecting the initial and goal configurations. Lozano-Perez studied this problem in configuration space, or C-space, a space in which a configuration of the piano maps to a point, a motion maps to a continuous curve, and the obstacles map to the C-obstacle, *i.e.*, the set corresponding to overlap between the piano and an obstacle [3]. The dimension of C-space is equal to the number of degrees of freedom of the system. The free space, or C-free, is what remains after removing the C-obstacle from C-space. In C-space, the motion planning problem becomes a path planning problem. That is, one must construct a continuous path connecting the initial and goal configurations that lies entirely within C-free. Theoretical results for the piano movers’ problem were first obtained by Schwartz, Sharir, and Hopcroft [17], [15]. They found that the problem is PSPACE hard, and proposed an algorithm based on Collins’ decomposition to find a path. Since the worst-case running time of Collins’ decomposition algorithm is doubly exponential in the dimension of C-space, it is impractical.

The more complex generalized movers’ problem, is the problem in which there are multiple rigid bodies moving simultaneously in a workspace. The bodies are the links of one or more robots, and thus may be required to obey constraints corresponding to their kinematic structures and joint limits. Given the importance of motion planning problem in robotics, researchers worked to find more efficient algorithms despite the depressing complexity results found earlier. The most efficient exact method known is Canny’s algorithm, which has time complexity that is only singly exponential in the

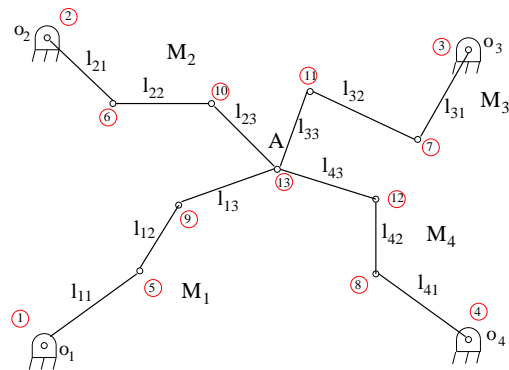


Fig. 1. Star-shaped manipulator with  $k = 4$ .

dimension of C-space [24]. He also made the important observation that this bound is worst-case optimal, since the worst-case number of components in C-space is exponential in its dimension. Canny’s algorithm is very difficult to implement - to date no full implementation exists.

In the 1990’s, the intractability of exact motion planning for general problems stimulated a paradigm shift to randomized methods. The method of Barraquand and Latombe combined potential field methods with random walk [13]. In essence, a potential field method defines an artificial potential field on C-space such that the goal configuration is the global minimum of the potential function and no saddle points or other local minima exist. When the function has this property, motion planning can be done by any gradient following algorithm. An important class of such functions are navigation functions [2], [7], [9]. Ideally, the potential function will be a function of the goal configuration, and the global minimum property will hold for all possible goal configurations. Since such potential functions can be difficult to design, Barraquand and Latombe suggested the use of random walks to escape local minima [13]. This modification yielded a method that is practically effective and probabilistically complete.

When possibly many motion planning queries must be handled for a single static environment, a different type of randomized method has been found to be more efficient than rerunning the Barraquand-Latombe algorithm for each query. The probabilistic roadmap method (PRM) of Kavraki *et. al* [26], is an easy-to-implement randomized version of Canny’s [24].

Because PRMs have been successful in solving problems in

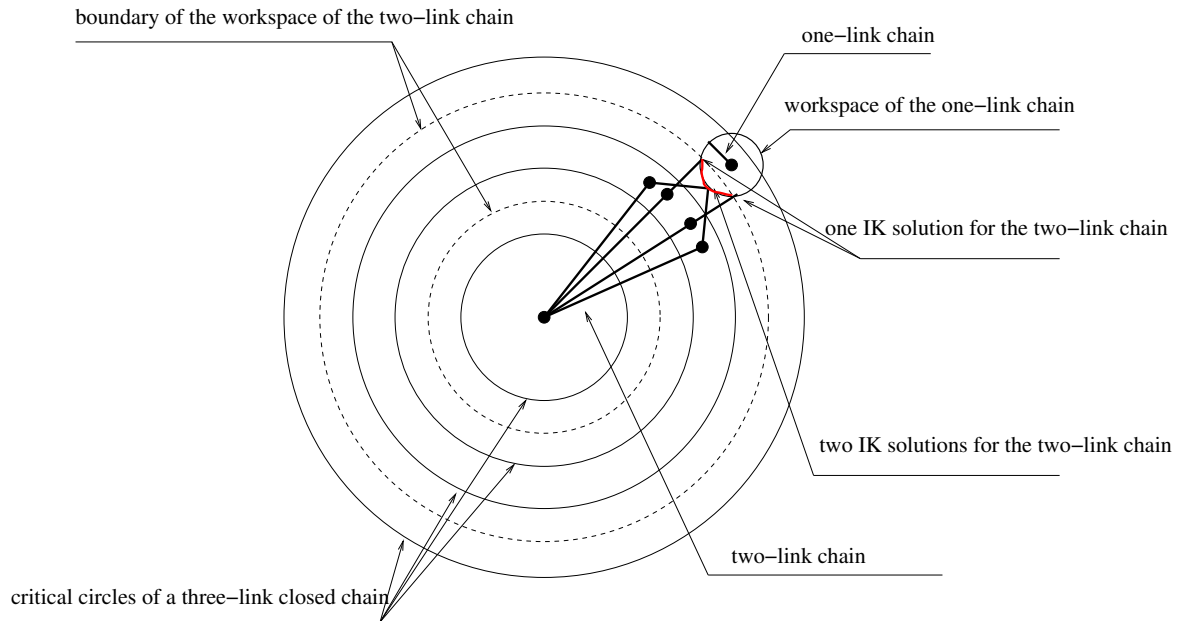


Fig. 2. Inverse kinematics of a three-link serial chain.

C-spaces with dimension approaching 100, many researchers have worked to make the method more efficient (e.g., [19], [20], [21]) and to modify it to solve more challenging types of problems, such as those with closed kinematic loops, nonholonomic constraints, dynamics, and intermittent contact (e.g., [30], [18], [1], [22], [23], [16]).

In this paper, we are particularly interested in planar *star-shaped manipulators*. These manipulators are formed by joining  $k$  planar “legs” to a common point (like the thorax of an insect) and then fixing the “feet” to the ground. The result is a planar parallel manipulator with  $k - 1$  independent closed loops. They are important because they arise in parallel manipulators, walking robots, and dexterous manipulation, and motion plans are difficult to obtain using PRMs. In such systems, C-space is often most naturally viewed as a lower-dimensional space embedded in an ambient space (typically the joint space). The embedding results from equality constraints corresponding to kinematic loop closure. In such settings, it is difficult to obtain an explicit description of C-space with minimal number of parameters and a suitable metric to guide sample generation. These problems make it difficult to construct a roadmap with the requisite properties, and hence difficult to solve motion planning problems for systems with kinematic loops using PRMs. The RLG (random loop generator) method [5], [6] improves the sampling techniques through estimating the regions of sampling parameters. However, its efficiency relies on the accuracy of the estimation, which often varies case by case. Moreover, it ignores the global structure of C-space, and may fail to sample globally important regions.

The difficulties associated with applying randomized motion planning methods to manipulators with closed chains and the availability of new results in topology [12], [25], [28], [10] have recently led to renewed interest in exact planning algorithms. Trinkle and Milgram derived some topological

properties of the C-spaces (the number of components and the structures of the components) of single-loop closed chains with spherical joints in a workspace *without* obstacles [29], [28]. These properties drove the design of a complete, polynomial-time motion planning algorithm that works roughly as follows.

- 1) Choose a subset  $\mathcal{A}$  of the links that can be positioned arbitrarily, and yet the remaining links can close the loop;
- 2) Move the links in  $\mathcal{A}$  to their goal orientations along an arbitrary path while maintaining loop closure;
- 3) Permanently fix the orientations of the links in  $\mathcal{A}$ ;
- 4) Repeat until all link orientations are fixed.

The main result that guided the algorithm’s design is Theorem 2 in [29]. In generic cases, the C-space is the union of manifolds that are products of spheres and intervals. The joint coordinates corresponding to the spheres are those that can contribute to the subset  $\mathcal{A}$  mentioned above and the structure of the C-space suggests a local parametrization for each step.

Here, the previous methods for C-space connectivity analysis are extended to planar star-shaped manipulators with revolute joints. These manipulators have a common junction point and  $k$  ( $k > 0$ ) legs connecting the junction to the fixed base. So the manipulator is in general subject to  $2(k - 1)$  independent nonlinear constraints, under which the workspace of the thorax and the C-space of the manipulator assume more complex combinatorial structures than single-loop closed chains. Following a topological analysis of the global structure of C-space (i.e., the structure of the inverse kinematics of the manipulator), the motion planning problem is solved completely in polynomial time. Furthermore since we consider only a point end-effector, the direct kinematics is straightforward while the inverse kinematics is more complex. Thus, while for most parallel mechanisms using C-space as a mean for path planning should be carefully considered, here our approach is natural.

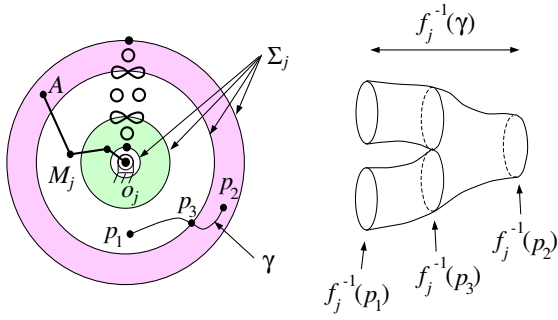


Fig. 3. **Left:** The workspace  $W_j$  of a three-link open chain  $M_j$  based at  $o_j$ . The critical set  $\Sigma_j$  of the kinematic map  $f_j$  is four concentric circles. The small circles, figure eights, and points at 12 o'clock show the topology of the C-space  $\tilde{\mathcal{C}}_j(p)$  of the leg when its endpoint is fixed at a point in one of the seven regions delineated by the critical circles (one of the four circles or one of the three open annular regions between them). **Right:** The inverse image of the curve  $\gamma$  - a “pair of pants.”

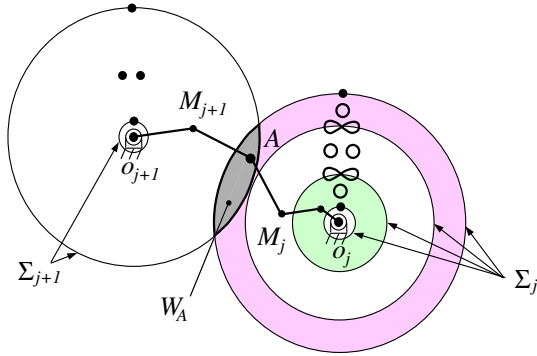


Fig. 4. The workspace  $W_A$  of  $A$  for a star-shaped manipulator with  $k = 2$  is the intersection of the workspaces of  $A$  for each leg considered separately. The critical set  $\Sigma$  is composed of the black circular arcs where they bound or intersect the gray area.

Note that this paper is aimed at possibly more complex macromolecules with non-covalent bonds (not just manipulators) for which the number of legs and links in each leg may be very large [4]. So such a polynomial-complex algorithm would play a key role in several issues in structural biology, such as structure prediction in protein folding and binding, and study of protein mobility in folded states. In these applications, we are interested in the robot motion planning problem without considering the control and sensor issues.

The main contributions of this paper are two folds. First, we establish the global connectivity of the C-space of star-shaped manipulators via a combination of the cell decomposition of workspace and the structure of the C-space at points in all cells. Second, the global connectivity result of C-space only suggests an exponential algorithm for path existence, which makes the motion planning formidable for macromolecules with a large number of links. In this paper we propose novel techniques for path existence that avoids the exponential complexity.

This paper is organized as follows. In Section III, kinematics and singularities of the manipulator are analyzed. In Section

IV, necessary and sufficient conditions for C-space connectivity and path existence are derived, based on which a complete polynomial-time algorithm is developed in Section V. Section VI addresses path optimization and robustness issues. Section VII shows simulation results that tests the effectiveness of our algorithm. Section VIII discusses the key difference between our algorithm and the others. Finally IX ends this paper with a brief conclusion.

## II. NOTATION

Manipulator Notation	
$M$	- Manipulator
$A$	- Root junction or thorax of $M$
$o_i$	- Grounding point of foot $i$ of $M$
$M_j$	- Leg $j$ of $M$ with foot fixed at $o_j$ and other end free, $j = 1, \dots, k$
$n_j$	- Number of links in $M_j$
$l_{j,i}$	- Length of link $i$ of $M_j$ ; $i = 1, \dots, n_j$
$\theta_{j,i}$	- Angle of link $i$ relative to link $i - 1$
$\tilde{M}_j(p)$	- Leg $j$ of $M$ with foot fixed at $o_j$ and other end fixed at $p$
$\tilde{M}(p)$	- Manipulator with $A$ fixed at $p$
$L_j$	- Sum of lengths of links of $\tilde{M}_j(p)$
$L_{j,0}$	- Sum of lengths of links of $M_j$
$\mathcal{L}_j(p)$	- A set of long links of $\tilde{M}_j(p)$
$ \mathcal{L}_j^*(p) $	- Number of long links of $\tilde{M}_j(p)$
Workspace Notation	
$W_A$	- Workspace of $A$
$dU_i$	- Cell of dimension $d$ of $W_A$
$p$	- Point in the plane of $M$
$\gamma = p(t)$	- Curve in the plane of $M$
$f$	- Kinematic map of $A$
$f_j$	- Kinematic map of endpoint of $M_j$
$\Sigma$	- Critical set of $f$ in $W_A$
$\Sigma_j$	- Critical set of $f_j$
Configuration Space (C-space) Notation	
$\mathcal{C}$	- C-space of $M$
$\tilde{\mathcal{C}}(p)$	- C-space of $\tilde{M}(p)$
$\mathcal{C}_j$	- C-space of $M_j$
$\tilde{\mathcal{C}}_j(p)$	- C-space of $\tilde{M}_j(p)$
$c$	- Point in C-space

## III. PRELIMINARIES

A star-shaped manipulator is composed of  $k$  serial chains with all revolute joints (see Fig. 1). Leg  $M_j$  is composed of  $n_j$  links of lengths  $l_{j,i}$ ,  $i = 1, \dots, n_j$  and joint angles  $\theta_{j,i}$ ,  $i = 1, \dots, n_j$ . At one end (the foot),  $M_j$  is connected to ground by a revolute joint fixed at the point  $o_j$ . At the other end, it is connected by another revolute joint to a junction point denoted by  $A$ . Note that when  $k$  is one, a star-shaped manipulator is an open serial chain. When  $k$  is two, it is a single-loop closed chain.

Assuming that the foot of  $M_j$  is fixed at  $o_j$ , let  $f_j(\Theta_j) = p$  denote the kinematic map of  $M_j$ , where  $\Theta_j = (\theta_{j,1}, \dots, \theta_{j,n_j})$  is the tuple of joint angles, and  $p$  is the location of the endpoint of the leg (the thorax end). When

$M_j$  is detached from the junction  $A$ , the image of its joint space is the reachable set of positions of the free end of the leg, called the workspace  $W_j$ . In the absence of joint limits, the workspace  $W_j$  is an annulus if and only if there exists one link with length strictly greater than the sum of all the other link lengths. Otherwise it is a disk. Clearly, the workspace  $W_A$  of  $A$  when all the legs are connected to  $A$  is given by:

$$W_A = \bigcap_{j=1}^k W_j. \quad (1)$$

In our study of  $\mathcal{C}$ , it will be convenient to refer to several other C-spaces. The C-space of leg  $M_j$  when detached from the rest of the manipulator will be denoted by  $\mathcal{C}_j$ . When the endpoint is fixed at the point  $p$ , leg  $j$  will be denoted by  $\tilde{M}_j(p)$ , where the tilde is used to emphasize the fact that the endpoint has been fixed. Note that  $\tilde{M}_j(p)$  is a single-loop planar closed chain, about which much is known (see [29]), including global structural properties of its C-space, denoted by  $\tilde{\mathcal{C}}_j(p) = f_j^{-1}(p)$ . When the junction  $A$  of a star-shaped manipulator is fixed at point  $p$ , its C-space will be denoted by  $\tilde{\mathcal{C}}(p)$ . Since collisions are ignored, the motions of the legs are independent, and therefore the C-space of the manipulator (with fixed junction) is the product of the C-spaces of the legs with all endpoints fixed at  $p$ :

$$\left. \begin{aligned} \tilde{\mathcal{C}}(p) &= \tilde{\mathcal{C}}_1(p) \times \cdots \times \tilde{\mathcal{C}}_k(p) \\ &= f_1^{-1}(p) \times \cdots \times f_k^{-1}(p) \\ &= f^{-1}(p) \end{aligned} \right\} \quad (2)$$

where by analogy,  $f$  is a total kinematic map of the star-shaped manipulator. Loosely speaking, the union of the C-spaces  $\tilde{\mathcal{C}}(p)$  at each point  $p$  in  $W_A$  gives the C-space of a star-shaped manipulator:

$$\mathcal{C} = \bigcup_{p \in W_A} \tilde{\mathcal{C}}(p). \quad (3)$$

Several properties of the C-spaces  $\mathcal{C}_j$  and  $\tilde{\mathcal{C}}_j(p)$  are highly relevant and so are reviewed here before analyzing the C-space of star-shaped manipulators. It is well known that the C-space of  $M_j$  is a product of circles (*i.e.*,  $\mathcal{C}_j = (S^1)^{n_j}$ )<sup>1</sup>. The workspace  $W_j$  contains a critical set  $\Sigma_j$  which is composed of all points  $p$  in  $W_j$  for which the Jacobian of the kinematic map  $Df_j(\Theta_j)$  drops rank for some  $\Theta_j \in f_j^{-1}(p)$ . These points form concentric circles of radii  $|l_{j,1} \pm l_{j,2} \pm \cdots \pm l_{j,n_j}|$ , as shown in Fig 3. When  $A$  coincides with a point in  $\Sigma_j$ , the links can be arranged such that they are all colinear, in which case the number of instantaneous degrees of freedom of the endpoint of the leg is reduced from two to one.

Now consider the case where the endpoint of leg  $j$  is fixed to the point  $p$ . In other words, we are interested in the C-space  $\tilde{\mathcal{C}}_j(p)$  of  $\tilde{M}_j(p)$ , which amounts to calculating the inverse kinematics (IK)  $f_j^{-1}(p)$ . The structure of  $f_j^{-1}(p)$  has been established in [14] for four-link single-loop closed chains, and in [29], [28] for chains with an arbitrary number of links.

Next, we compute  $f_j^{-1}(p)$  for a three-link serial chain to explain the basic idea used in [29], [28] for analyzing the IK

map of a closed chain with an arbitrary number of links. As shown in Fig. 2, we begin with the IK of a two-link serial chain. Each point in the workspace could have 0,1, or 2 IK solutions, and the set of points with constant number of IK solutions forms annular regions separated by the critical set of this chain. The IK of a three-link serial chain is then deduced by breaking the chain into a two-link serial chain and a one-link serial chain, and taking the union of the IK solutions of the two-link chain for all points in the workspace of the one-link chain. It is easy to check that for points in the outer most annular region in the workspace of the three-link chain, the workspace of the one-link chain (a circle) always intersects with the outer-most critical circle of the two-link chain at two points, indicating that the IK of this point is the union of two curve segments with a pair of endpoints identified, respectively, *i.e.*, a circle. The inverse kinematics for points in other regions can be derived similarly. The results are shown in Fig. 3. In the 12 o'clock position, points, circles, and figure eights are drawn to represent the global structures of  $\tilde{\mathcal{C}}_j(p)$  in the seven regions of  $W_j$ . Specifically, when  $A$  is fixed to a point  $p$  on the outer-most critical circle,  $\tilde{\mathcal{C}}_j(p)$  is a single point. For  $p$  fixed to any point in the largest open annular region, C-space is a single circle. Continuing inward, the possible C-space types are a figure eight (on the second largest critical circle), two disconnected circles, a figure eight again, a single circle, and a single point (on the inner-most critical circle).

[29] summarizes several important properties about  $\mathcal{C}_j(p)$  with an arbitrary number of links. Those that will be particularly useful in the analysis of star-shaped manipulators follow. First, the connectivity of  $\tilde{\mathcal{C}}_j(p)$  is uniquely determined by the number of "long links." Consider the augmented link set composed of the links of  $M_j$  and  $\overline{\partial_j p}$ , which will be called the fixed base link with length denoted by  $l_{j,0}$ . Let  $L_j$  be the sum of all the link lengths including the fixed base link (*i.e.*,  $L_j = \sum_{i=0}^{n_j} l_{j,i}$ ). Further, let  $\mathcal{L}_j(p)$  be a subset of  $\{0, 1, \dots, n_j\}$  such that  $l_{j,\alpha} + l_{j,\beta} > L_j/2$ ;  $\alpha, \beta \in \mathcal{L}_j(p)$ ,  $\alpha \neq \beta$ . Over all such sets, let  $\mathcal{L}_j^*(p)$  be a set of maximal cardinality. Then the number of long links of  $\tilde{M}_j(p)$  is defined as  $|\mathcal{L}_j^*(p)|$ , where  $|\cdot|$  denotes set cardinality.

**Lemma 1: Kapovich and Milson [25], Trinkle and Milgram [29]**

The C-space  $\tilde{\mathcal{C}}_j(p) = f_j^{-1}(p)$  has two components if and only if  $|\mathcal{L}_j^*(p)| = 3$ , and is connected if and only if  $|\mathcal{L}_j^*(p)| = 2$  or 0. No other cardinality is possible.

Let us return to the discussion of Fig. 3. Viewing  $W_j$  as a base manifold and the C-space corresponding to each end point location as a fibre, it is apparent that the critical set  $\Sigma_j$  partitions  $W_j$  into regions over which the C-spaces  $\tilde{\mathcal{C}}_j(p)$  form a trivial fibration. The implications of this observation are useful in determining the C-space of more complicated mechanisms. Consider a modification to  $\tilde{M}_j(p)$  that allows the endpoint to move along a one-dimensional curve segment  $\gamma$  within  $W_j$ . Then as long as  $\gamma$  is entirely contained in one of the regions defined by the critical circles,  $\tilde{\mathcal{C}}_j(\gamma) = \tilde{\mathcal{C}}_j(p) \times I$ , where  $I$  is the interval. If  $\gamma$  crosses a critical circle transversally, then  $\tilde{\mathcal{C}}_j(\gamma) = (\tilde{\mathcal{C}}_j(p_1) \times I) \cup \tilde{\mathcal{C}}_j(p_3) \cup (\tilde{\mathcal{C}}_j(p_2) \times I)$ , where  $p_1$  is a point in one of the two open annular regions containing  $\gamma$ ,  $p_2$

<sup>1</sup>Recall the assumption of no joint limits.

is a point in the other, and  $p_3$  is a point on the critical circle crossed by  $\gamma$ , and  $\cup$  denotes the standard “gluing” operation. In Fig. 3, an example  $\gamma$  and the corresponding C-space  $\tilde{\mathcal{C}}_j(\gamma)$  are shown.

#### IV. ANALYSIS OF STAR-SHAPED MANIPULATORS

For star-shaped manipulators with one or two legs, the global topological properties of the C-space  $\mathcal{C}$  are fully understood (for one, see [27]; for two, see [29], [28]). The goals of this section are to study the global properties of  $\mathcal{C}$  when  $M$  has more than two legs and to derive necessary and sufficient conditions for solution existence to the motion planning problem.

1) *Local Analysis:* As a direct generalization of the critical set of a single leg, we define the critical set of a star-shaped manipulator as a subset  $\Sigma$  of  $W_A$  such that for every  $p \in \Sigma$ , there exists a configuration  $c$  such that at least one of the Jacobians  $\{Df_1(c), \dots, Df_k(c)\}$  drops rank. By definition we have:

$$\Sigma = \left( \bigcup_{i=1}^k \Sigma_i \right) \cap W_A. \quad (4)$$

An advantage of this definition is that  $\Sigma$  can be used to stratify  $W_A$  such that each stratum is trivially fibred. Figure 4 shows a star-shaped manipulator with two legs. The critical set  $\Sigma$  is the boundary of the lune formed by the intersection of the outer critical circles of their individual workspaces. For every point interior to the lune, the fibre is two circles (the direct product of two points with one circle). The fibres associated to the vertices of the lune are single points, which correspond to simultaneous full extension of the two legs.

Fig. 5 shows a possible workspace for a star-shaped manipulator with three legs. The critical set defines 65 distinct sets  ${}^dU_i$  of varying dimension  $d$ , where  $i$  is an arbitrarily assigned index that simply counts components. We will refer to these sets as *chambers*. There are 12 two-dimensional, 32 one-dimensional, and 21 zero-dimensional chambers, each of which is trivially fibred. Removing the  ${}^0U_i$  from  $\Sigma$  partitions it into open one-dimensional chambers  ${}^1U_i$ ,  $i = 1, \dots, {}^1m$ . Removing  ${}^0U_i$  and  ${}^1U_i$  from  $W_A$  yields open two-dimensional sets  ${}^2U_i$ ,  $i = 1, \dots, {}^2m$ , for which the following relationships hold:

$$\Sigma = \left( \bigcup_{i=1}^{{}^0m} {}^0U_i \right) \cup \left( \bigcup_{i=1}^{{}^1m} {}^1U_i \right) \quad (5)$$

$$W_A - \Sigma = \bigcup_{i=1}^{{}^2m} {}^2U_i. \quad (6)$$

**Proposition. 1:** For all  $d = 0, 1, 2$  and  $i$ ,  $f^{-1}({}^dU_i) = {}^dU_i \times f^{-1}(p)$ , where  $p$  is any point in  ${}^dU_i$  and the operator  $\times$  denotes the direct product. Gluing the  $f^{-1}({}^dU_i)$  for all  $i$  and  $d$  gives the total C-space  $\mathcal{C}$ .

**Proof:** When  $d = 0$ ,  ${}^0U_i$  contains a single point, the result follows. When  $d = 1$ ,  ${}^1U_i$  belongs to one critical circle of one leg, say  $\tilde{M}_j$ . Any two points  $p_1, p_2 \in {}^1U_i$  are related by a

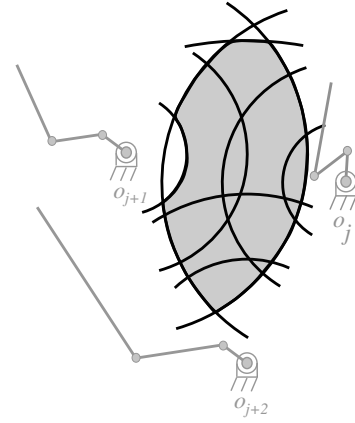


Fig. 5. Workspace (shaded gray) of a star-shaped manipulator with three legs. The critical set partitions  $W_A$  into 12 two-dimensional, 32 one-dimensional, and 21 zero-dimensional chambers.

Euclidean rotation  $p_2 - o_j = R(p_1 - o_j)$ , indicating that  $\tilde{\mathcal{C}}_j(p_1)$  and  $\tilde{\mathcal{C}}_j(p_2)$  are homotopic. Thus  $\tilde{\mathcal{C}}_j(p)$  for all  $p \in {}^1U_i$  have equivalent topological structure. For the other legs  $\tilde{M}_l$ ,  $l \neq j$ , according to [28] (Lemma 6.1 and Corollary 6.5)  $\tilde{\mathcal{C}}_l(p)$  for all  $p \in {}^1U_i$  have equivalent topological structures as  ${}^1U_i$  is free of critical points of  $\tilde{M}_l(p)$ . Thus  $f^{-1}(p) = \tilde{\mathcal{C}}_1(p) \times \dots \times \tilde{\mathcal{C}}_k(p)$  for all  $p \in {}^1U_i$  have equivalent topological structures. The case when  $d = 2$  can be proved by applying Lemma 6.1 and Corollary 6.5 of [28] to all legs. ■

Proposition 1 and the fact that  ${}^dU_i$  is a simply connected set, reveal that each component of  $f^{-1}({}^dU_i)$  is a direct product of one component of  $\tilde{\mathcal{C}}_j(p)$ ,  $j = 1, \dots, k$ , with a  $d$ -dimensional disk. Using  $|\mathcal{L}_j^*(p)|$ ,  $j = 1, \dots, k$  and Lemma 1, one can show that the number of components of  $f^{-1}({}^dU_i)$  is  $2^{k_0}$ , where  $k_0 \leq k$  is the number of legs for which  $|\mathcal{L}_j^*(p)| = 3$ .

2) *Local Path Existence:* Before considering the global path existence problem, consider motion planning between two valid configurations  $c_{\text{init}}$  and  $c_{\text{goal}}$  for which the junction  $A$  lies in the same chamber. Since the fibre over every point in  ${}^dU_i$  is equivalent, path existence amounts to checking the component memberships of the configurations  $c_{\text{init}}$  and  $c_{\text{goal}}$ .

For a single leg  $\tilde{M}_j(p)$ , if the number of long links  $|\mathcal{L}_j^*(p)|$  is not three, then any two configurations of  $\tilde{M}_j(p)$  are in the same component. When  $|\mathcal{L}_j^*(p)| = 3$ , choose any two long links and test the sign of the angle between them (with full extension taken as zero). There are two possible signs, one corresponding to *elbow-up* and the other to *elbow-down*. If for two distinct configurations of  $\tilde{M}_j$ ,  $A$  lies in the same chamber, there is a continuous motion between them while keeping  $A$  in this chamber, if and only if the elbow sign is the same at both configurations (naturally, one must perform the sign test with the same two links and in the same order for both configurations). Considering all the legs together, a continuous motion of  $A$  in  ${}^dU_i$  exists if and only if a motion exists for each leg individually. The previous discussion serves to prove the following result.

**Proposition. 2:** Restricted to  $f^{-1}({}^dU_i)$ , two configurations  $c_1, c_2 \in f^{-1}({}^dU_i)$  are path connected if and only if for each

leg  $\tilde{M}_j$  with  $|\mathcal{L}_j^*| = 3$  in  ${}^dU_i$ , the elbow angle of  $\tilde{M}_j$  has the same sign at  $c_1$  and  $c_2$ .

Proposition 2 completely solves the path existence problem if  $W_A$  consists of a single chamber. However, things become complex when  $W_A$  has more than one chamber.

3) *Singular Set and Global C-space Analysis:* Recall that the C-space  $\mathcal{C}$  is a union of  $f^{-1}({}^dU_i)$ ,  $d \in \{0, 1, 2\}$ ,  $i = 1, \dots, {}^d m$  and that  $f^{-1}(p)$ ,  $p \in {}^dU_i$  for  $d \neq 2$  and all  $i$  is a set containing at least a singularity of  $f$ . Combining the local C-space and singular set analysis yields the global structure of C-space.

**Proposition. 3:** For all  $p \in \Sigma_j$ ,  $f_j^{-1}(p)$  is a singular set containing isolated singularities. If a singularity separates its neighborhood  $V$  in  $f_j^{-1}(p)$ , then it is these singularities which glue the two separated components in  $f_j^{-1}(q)$  where  $q \in W_A - \Sigma_j$  is a point sufficiently close to  $p$ .

**Proof:** First it is obvious that  $f_j^{-1}(p)$  contains isolated singularities for there are finite ways to colinearize all the links of a close chain. Second, let

$$\gamma : (-\varepsilon, \varepsilon) \rightarrow W_A, \gamma(0) = p$$

be a curve that is transverse to  $\Sigma_j$ . According to Corollary 6.6 of [28], the distance function  $s(\gamma(t)) = \int_0^t |\dot{\gamma}| dt$  defines a Morse function on  $f_j^{-1}(\gamma)$

$$s \circ f_j : f_j^{-1}(\gamma) \rightarrow \mathbb{R}.$$

Note that 0 is a singular value of  $s \circ f_j$  and the isolated singularities of  $f_j^{-1}(p)$  are also singularities of  $s \circ f_j$ . The result of Morse theory applying to  $s \circ f_j$  yields that  $(s \circ f_j)^{-1}(0) = f_j^{-1}(p)$  is given by attaching a handle to  $(s \circ f_j)^{-1}(\varepsilon_0) = f_j^{-1}(q)$  for a sufficiently small  $\varepsilon_0$  and  $q$  a point sufficiently close to  $p$ . The Proposition follows. ■

Next, we establish necessary and sufficient conditions for the connectivity of  $\mathcal{C}$ . Let  $J$  be the index set such that for all  $j \in J$ ,  $|\mathcal{L}_j^*| = 3$  for at least one chamber  ${}^dU_i$ . We prove the following theorem.

**Theorem 1:** Suppose  $W_A = \bigcup_{d=0}^2 \left( \bigcup_{i=1}^m {}^dU_i \right)$ . Then  $\mathcal{C} = f^{-1}(W_A)$  is connected if and only if:

- 1)  $W_A$  is connected;
- 2)  $\Sigma_j \cap W_A \neq \emptyset$  for all  $j \in J$ .

**Proof:** (i) “Necessity:” Since  $\mathcal{C}$  is a fibration of the base manifold  $W_A$ , it can have one component only when  $W_A$  has one component. Thus item 1 of Theorem 1 is required. Second, in order that  $\mathcal{C}$  be connected, for each leg  $M_j$  restricted to  $W_A$ , the C-space  $\tilde{\mathcal{C}}_j(W_A) = f_j^{-1}(W_A)$  must be connected. By definition, for all  $j \in J$ , there exists a chamber  ${}^dU_i$  such that  $|\mathcal{L}_j^*| = 3$ . The result of Proposition 3 means that  $\tilde{\mathcal{C}}_j(W_A)$  is connected only if  $W_A \cap \Sigma_j \neq \emptyset$ .

(ii) “Sufficiency:” Item 1 and 2 imply that  $\tilde{\mathcal{C}}_j(W_A)$  are path connected for all  $j$ . Moreover,  $\mathcal{C}$  is a fibration over  $W_A$ . The result follows. ■

Fig. 6 illustrates the global connectivity for an example  $W_A$  corresponding to a star-shaped manipulator with two legs and

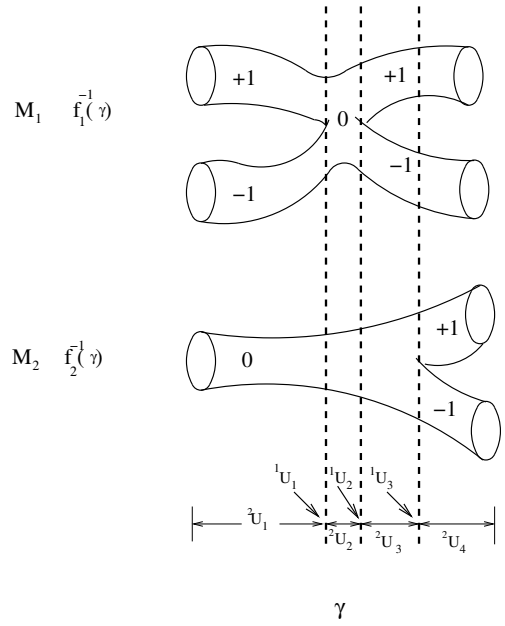


Fig. 6. C-space of a star-shape manipulator with two legs. For simplicity, only the portion of  $f^{-1}(\gamma)$  is shown, where  $\gamma$  is a continuous curve in  $W_A$  that visits all chambers.

a workspace for which there are two chambers  ${}^2U_1$  and  ${}^2U_3$  where leg 1 has three long links and another chamber  ${}^2U_4$  where both legs have three long links. Among these chambers,  ${}^1U_1$  and  ${}^1U_2$  belong to  $\Sigma_1$ , and  ${}^1U_3$  belongs to  $\Sigma_2$ . According to Theorem 1, the C-space is path connected. In this example, the  $\mathcal{C}$  is the product of the two structures shown.

**Corollary 1:** Two configurations  $c_1$  and  $c_2$  of a star-shaped manipulator are in the same component if and only if

- 1)  $f(c_1)$  and  $f(c_2)$  are in the same component of  $W_A$ ;
- 2) For each leg  $j$  with  $|\mathcal{L}_j^*| = 3$  for all chambers  ${}^dU_i$  in the component of  $W_A$  which contains  $f(c_1)$  and  $f(c_2)$ , the elbow sign is same at both  $c_1$  and  $c_2$ .

**Remark 1:** As a matter of fact,  $\Sigma$  completely determines the connectivity of C-space. When computing a path between two given configurations, often motions of the junction to points on  $\Sigma$  are incorporated to allow adjustment of leg-angle signs. However, inevitable deviations of the junction from  $\Sigma$  caused by numerical errors, make it impossible to adjust the sign of legs while fixing its end point. For these reasons, points in 2D chambers are preferred for sign adjustment.

## V. A POLYNOMIAL-TIME, EXACT, COMPLETE ALGORITHM

Our algorithm consists of two main routines, PathExists and ConstructPath. PathExists solves the path existence problem, i.e., determining if an initial and an goal configuration are path-connected, and ConstructPath constructs a path between them if there exists a path.

Notice that the C-space of a star-shaped manipulator could be very complex. Even the simple planar five-link single-loop closed chain, its C-space could be as complex as the connected sum of four torii [28]. So determining the path existence without using the C-space information is difficult. Our strategy

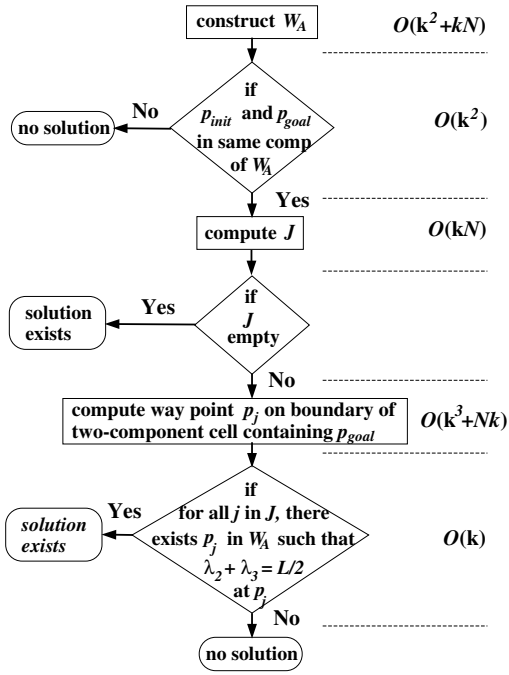


Fig. 7. Logical flow and complexity of the major steps of PathExists.

is to solve the path existence based on the set of critical circles  $\Sigma_j$  in the workspace, and then construct the path combining our knowledge of the workspace and the structure of the C-space of single-loop closed chains. We emphasize here that the problem is not just moving the junction point between an initial and a goal position, but moving the manipulator along with all its legs from an initial configuration to a goal configuration. So, the workspace information will be insufficient for path construction. In ConstructPath, we employ a move that changes the shape of a leg with its endpoint fixed in the workspace. This move, called the sign-adjust move, uses the knowledge of the C-space of a single-loop closed chain. Below we will show that the overall complexity of PathExists and ConstructPath is  $O(k^3 N^3)$ , where  $N$  is the maximum number of links in a leg and  $k$  is the number of legs. The polynomial complexity is key to the applications like folding of macromolecules, which can be modeled as a closed chain with large  $k$  and  $N$ .

The logical flow of PathExists is illustrated in Figure 7. Its input is the topology and link lengths of a star-shaped manipulator and two valid configurations,  $c_{\text{init}}$  and  $c_{\text{goal}}$ . The output is the answer to the path existence question.

The approach taken is to compute  $W_A$  and then, for each leg with its end point constrained to lie in  $W_A$ , to determine if its initial and goal configurations are path connected. Notice that  $W_j$  is either a disk or an annular region,  $W_A$  can be constructed by calculating the intersections between no more than  $2n$  circles. So constructing  $W_A$  is polynomial-complex. The most difficult issue is to check the path existence.

Since the C-space of a leg is guaranteed to be connected if one of its critical circles  $\Sigma_j$  intersects  $W_A$ , the most straight forward way to test connectivity is to explicitly perform the intersections. However, since there are as many as  $2^{n_j-1}$

critical circles, any algorithm based on this approach will have worst-case complexity that is at least exponential in  $N$ . The key contribution of PathExists is a polynomial-time algorithm for checking the existence of an intersection between  $W_A$  and a critical circles - even though there is an exponential number of these circles. Recall that if a leg has three long links, then it is impossible to move the leg so that the three long links change from an elbow-up configuration to an elbow-down configuration. The following algorithm constructs a novel polynomial-complex method that can determine if there is point in  $W_A$  in which the number of long links of a leg is not 3 (see Step 4 in PathExists).

**1. Construct  $W_A$**  We compute  $W_A$  in three steps.

**Step 1:** Compute the boundary circles of  $W_j$ . In general,  $W_j$  is an annulus. The radius of its outer boundary circle is  $r_{\text{max}} = \sum_{i=1}^{n_j} l_{j,i}$ , while that of its inner boundary circle,  $r_{\text{min}}$ , can be determined by comparing  $l_{\text{max}} := \max_i l_{j,i}$  and  $r_{\text{max}} - l_{\text{max}}$ . If  $l_{\text{max}} > r_{\text{max}} - l_{\text{max}}$ , then  $r_{\text{min}} = 2l_{\text{max}} - r_{\text{max}}$ , else,  $r_{\text{min}} = 0$ ;

**Step 2:** Decompose the whole plane into cells using all boundary circles of all legs (e.g., the line sweeping algorithm can do this), and construct the cell adjacency graph;

**Step 3:** Pick a point from the interior of each cell, compute its distance from each base point, and compare the distance with the radii of the two boundary circles of  $W_j$ . The set of cells which can be reached by all legs constitute  $W_A$ .

The complexity of this 2-D cell decomposition algorithm is  $O(k^2 + kN)$ .

**2. Are  $p_{\text{init}}$  and  $p_{\text{goal}}$  in same component of  $W_A$ ?** As an immediate consequence of the cell decomposition, this can be answered directly by searching the cell graph.

**3. Compute  $J$**  This step is used to filter out easy solution existence checks, based on the cardinality and members of the sets  $\mathcal{L}_j^*(p_{\text{init}})$  and  $\mathcal{L}_j^*(p_{\text{goal}})$ . For each leg  $\tilde{M}_j(p_{\text{init}})$ , compute  $L_j$  (see Section III) and find the three longest links of the set  $\{l_{j,0}, \dots, l_{j,n_j}\}$ . Denote these links by  $(p_{\text{init}}; \lambda_{j,1}, \lambda_{j,2}, \lambda_{j,3})$ . Do the same for  $(p_{\text{goal}})$  and define  $(p_{\text{goal}}; \lambda_{j,1}, \lambda_{j,2}, \lambda_{j,3})$ . This requires  $O(N)$  work. Finally,  $|\mathcal{L}_j^*(p_{(\cdot)})| = 3$  if and only if  $\lambda_{j,2} + \lambda_{j,3} > L_j/2$ . If  $\mathcal{L}_j^*(p_{\text{init}}) = \mathcal{L}_j^*(p_{\text{goal}})$  and  $|\mathcal{L}_j^*(p_{\text{init}})| = 3$ , and if the signs of the long links are different at  $c_{\text{init}}$  and  $c_{\text{goal}}$ , then add  $j$  into  $J$ . Computing  $J$  is  $O(kN)$ .

**4. Does the set of long links vary for all  $j \in J$ ?** If and only if  $q \in W_A$  exists such that  $\mathcal{L}_j^*(q) \neq \mathcal{L}_j^*(p_{\text{init}})$ , then it is possible to make the long links colinear and thus change the signs of their relative angles. This can be done by computing a point  $q \in W_A$  on the boundary of the cell that contains  $p_{\text{goal}}$  and keeps the same set  $\mathcal{L}_j^*(p)$  for all  $p$  in this cell. This boundary is characterized by  $\lambda_{j,2} + \lambda_{j,3} = L_j/2$ . Since  $l_{j,0}$  is the only link whose length varies along with  $p$ , this boundary must be one or two circles (called inner and outer circles, respectively) whose radii, denoted  $d_{\text{max}}$  and  $d_{\text{min}}$ , depend on the link lengths of the leg. Let  $L_{j,0} = \sum_{i=1}^{n_j} l_{j,i}$  and suppose the four longest links at  $p_{\text{goal}}$  are  $(\lambda_{j,1} > \lambda_{j,2} > \lambda_{j,3} > \lambda_{j,4})$  with  $\lambda_{j,2} + \lambda_{j,3} > L_j/2$ , we deduce the radii of the boundary circles for four different cases:

Case 1: if  $l_{j,0}(p_{\text{goal}}) = \lambda_{j,1}$ , then  $d_{\text{max}} = 2(\lambda_{j,2} + \lambda_{j,3}) - L_{j,0}$ ,

and  $d_{\min} = \max\{L_{j,0} - 2\lambda_{j,3}, 2(\lambda_{j,3} + \lambda_{j,4}) - L_{j,0}\}$ .  
Case 2: if  $l_{j,0}(p_{\text{goal}}) = \lambda_{j,2}$ ,  $d_{\max} = 2(\lambda_{j,1} + \lambda_{j,3}) - L_{j,0}$ ,  
and  $d_{\min} = \max\{L_{j,0} - 2\lambda_{j,3}, 2(\lambda_{j,3} + \lambda_{j,4}) - L_{j,0}\}$ .  
Case 3: if  $l_{j,0}(p_{\text{goal}}) = \lambda_{j,3}$ ,  $d_{\max} = 2(\lambda_{j,1} + \lambda_{j,2}) - L_{j,0}$ ,  
and  $d_{\min} = \max\{L_{j,0} - 2\lambda_{j,2}, 2(\lambda_{j,2} + \lambda_{j,4}) - L_{j,0}\}$ .  
Case 4: Otherwise,  $d_{\max} = \min\{2(\lambda_{j,2} + \lambda_{j,3}) - L_{j,0}, L_{j,0} - 2\lambda_{j,2}\}$ , and  $d_{\min} = 0$ .

If there is no overlap between the two boundary circles and the component of  $W_A$  that contains  $p_{\text{init}}$  and  $p_{\text{goal}}$ , then no path exists between  $c_{\text{init}}$  and  $c_{\text{goal}}$ . Otherwise, path exists and we obtain way points  $p_j$  for all legs  $j \in J$ . Computing  $d_{\max}$ ,  $d_{\min}$ , and the way points  $p_j$  is  $O(kN)$ .

The basic idea of `ConstructPath` is that when moving from  $c_{\text{init}}$  to  $c_{\text{goal}}$ , those legs  $j \in J$  may require a change in the signs of relative angles between long links, which is always possible at the way point  $p_j$  or other critical points of the corresponding leg. A natural approach then is to use two motion generation primitives: *accordion move* and *sign-adjust move*. The former moves the thorax endpoint (at  $A$ ) along a specified path segment with all legs moving compliantly so that all loop closures are maintained. The latter keeps the endpoint fixed at a way point  $q_j \in \Sigma_j$  (e.g.,  $q_j = p_j$  or other critical points) while moving leg  $j$  into a singular configuration and then to a nearby configuration with the sign of the relative angle between a pair of long links in this leg chosen to match those of  $c_{\text{goal}}$ .

Note that though  $q_j$  are in the critical set  $\Sigma_j$ , the configuration at which leg  $j$  approaches these points need not to be aligned. Without considering the control issue, a leg can be moved to a colinear configuration with the thorax fixed. Even if control is considered for the sign-adjust move, the thorax can still be maintained to be fixed by keeping all other legs not aligned in the vicinity of  $q_j$ .

The input of `ConstructPath` is  $W_A$  and its cell graph,  $c_{\text{init}}$ ,  $c_{\text{goal}}$ , and the set of way points  $p_j \in W_A$ ,  $j \in J$  computed during the execution of `PathExist`.

**1. Construct an initial path** `ConstructPath` explores the cell graph of  $W_A$ , and constructs a path in  $W_A$  connecting  $p_{\text{init}}$  to  $p_{\text{goal}}$  and visiting all of the way points. Since there are at most  $k$  way points, this can be done in  $O(k^3)$  time (the path has  $k + 1$  segments each with  $O(k^2)$  arcs).

**2. Construct *guards* and insert the guards into the path** Notice that when one accordion moves a leg in a cell in which the number of long links is not 3 (called one-component cell), neither the signs of concatenating angles, nor the sign between any pair of links in this leg will be kept invariant. Thus even if the desired sign between a pair of long links is adjusted at a way point, it still could change if the leg keeps moving in a one-component cell. For this reason, we set *guards* for legs which have three long links at  $p_{\text{goal}}$ . These are the set of points  $q_j$ , each of which is the last intersection point between the above constructed path in  $W_A$  and the boundary of the two-component cell of leg  $j$  containing  $p_{\text{goal}}$ . Thus the number of guards ( $q_j$ 's) may be more than the number of way points since the number of legs that have three long links at  $p_{\text{goal}}$  may be more than the cardinality of  $J$ . Next the *guards* are inserted into the path. Later when we construct the path in  $\mathcal{C}$ ,

sign-adjust moves are only performed at *guards*  $q_j$  (but not  $p_j$ ) for after that the thorax endpoint gets into the two-component cell and the sign between a pair of long links will not change during accordion moves, i.e., the leg will always remain in the right component of its C-space. Assuming each arc in the path is approximated by a fixed number of line segments, finding guards is  $O(k^3)$ .

**3. Accordion moves and sign-adjust moves** The path in  $\mathcal{C}$  then is produced by using accordion moves along the path and sign-adjust moves at the *guards*. At each *guard*, one checks the sign between a pair of long links of the corresponding leg. If it does not match the goal one, then the junction point is fixed while a sign-adjust move is executed, otherwise, the accordion move continues. Once  $A$  is coincident with  $p_{\text{goal}}$ , one is assured by the previous steps, that with  $A$  fixed at  $p_{\text{goal}}$ , the configuration of each leg is in the same component of its current C-space  $\tilde{\mathcal{C}}_j(p_{\text{goal}})$  as  $c_{\text{goal}}$ . The final move can be accomplished using a special accordion move algorithm found in [29]. At this stage, we remark that finding the set of way points  $p_j$  and planning an initial path visiting all  $p_j$  is necessary for otherwise, an arbitrary path between  $p_{\text{init}}$  and  $p_{\text{goal}}$  may not intersect the boundary of the two-component cell of a leg that contains  $p_{\text{goal}}$ .

The complexity of the accordion move algorithms reported in [29] are  $O(N^3)$ . Since the path has  $O(k^3)$  line segments the complexity of `ConstructPath` is  $O(k^3N^3)$ . Note that accordion move algorithms with the required behavior can be designed to be  $O(N^2)$ , so the complexity of `ConstructPath` could be reduced.

Overall, our path planning algorithm is  $O(k^3N^3)$ .

## VI. PATH OPTIMIZATION AND ROBUSTNESS

If a path between two given configurations exists, it is obvious that in our algorithm the choice of way points, and thus the path between the two configurations, is not unique. So a natural problem is path optimization with respect to meaningful metrics such as path length and singularity avoidance. Basically we say that many possible optimization objectives are potentially useful, but we consider the shortest path in this section. Notice that the way points are necessary for successively constructing a path from  $c_{\text{init}}$  to  $c_{\text{goal}}$  since an arbitrary chosen path of the thorax from  $p_{\text{init}}$  to  $p_{\text{goal}}$  (like the line connecting them) will either go out of  $W_A$ , or have no intersection with the critical set  $\Sigma_j$ , in which a sign-adjust move is required for a leg. Thus the optimization problem arises in the choice of way points, the order of the way points, and the path between two consecutive way points.

One may also take into consideration parallel singularities (cf. [31]) and try to avoid them as much as possible by minimizing the number of singularity crossings. More precisely this may be done for example by first clustering singularity regions (see [32]) and then choosing the way points for the corresponding path so that it has the minimal number of crossings with these regions. Moreover, the paths or trajectories (i.e. a path with temporal relations as well as the geometrical ones) between the way points should be chosen in the proper way (cf. [33]).



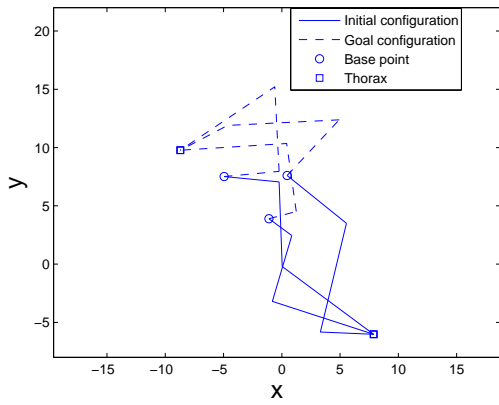


Fig. 8. Initial and goal configurations (see Extension 2 for the entire video)

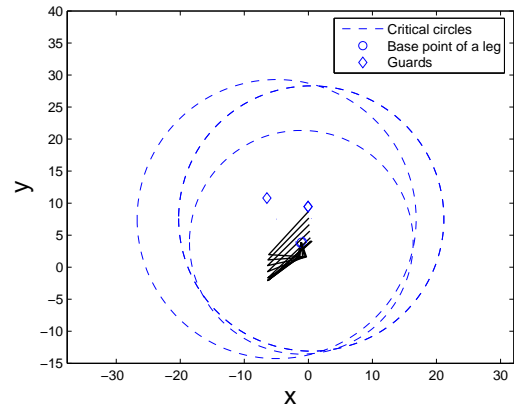


Fig. 11. Motion of leg 1: step 3.

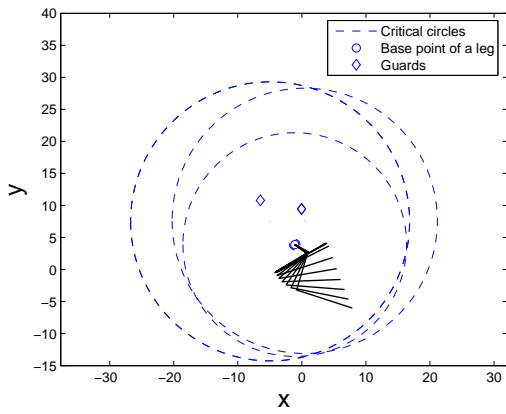


Fig. 9. Motion of leg 1: step 1.

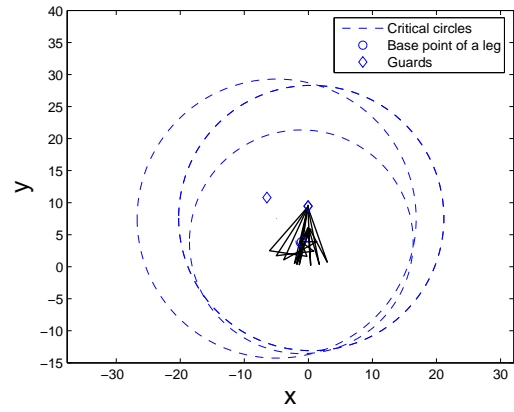


Fig. 12. Motion of leg 1: step 4.

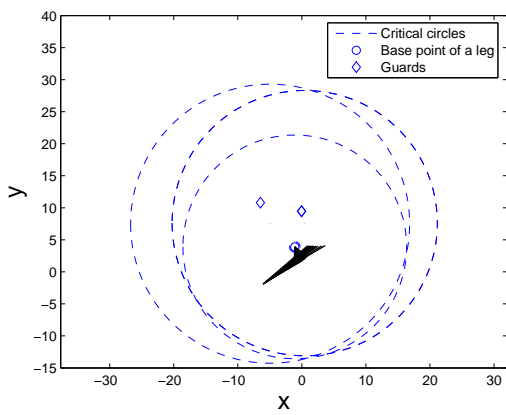


Fig. 10. Motion of leg 1: step 2.

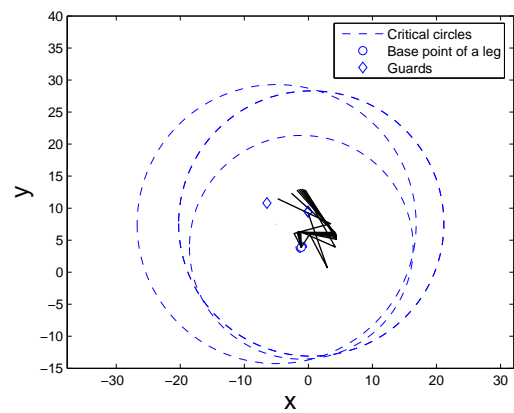


Fig. 13. Motion of leg 1: step 5.

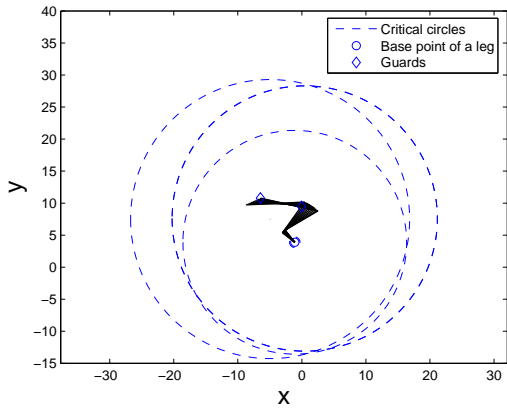


Fig. 14. Motion of leg 1: step 6.

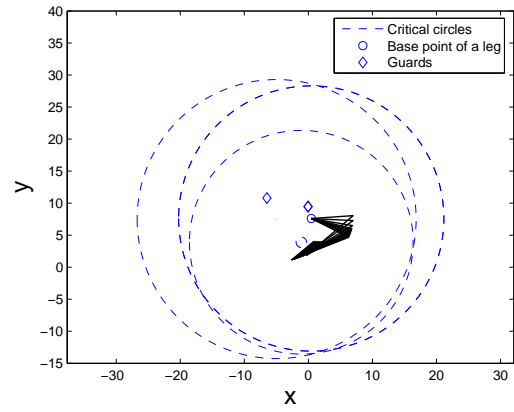


Fig. 17. Motion of leg 2: step 2.

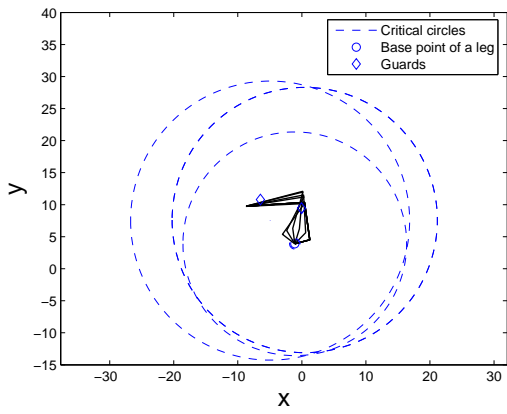


Fig. 15. Motion of leg 1: step 7.

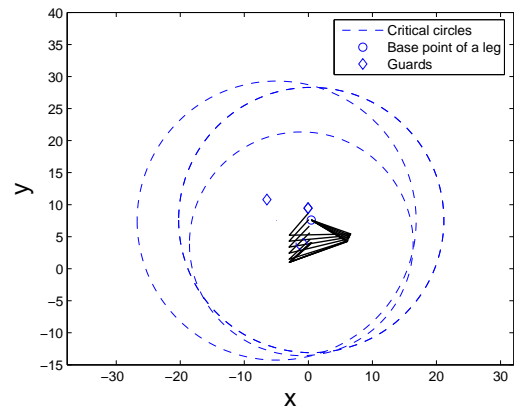


Fig. 18. Motion of leg 2: step 3.

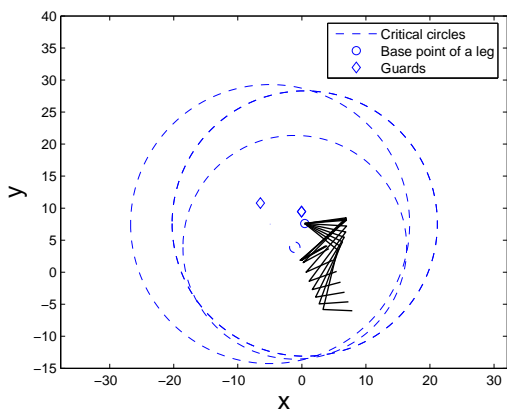


Fig. 16. Motion of leg 2: step 1.

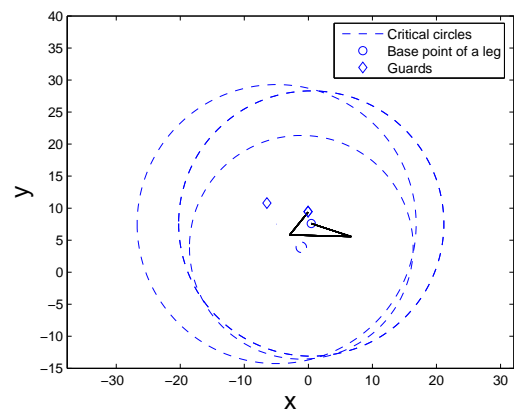


Fig. 19. Motion of leg 2: step 4.

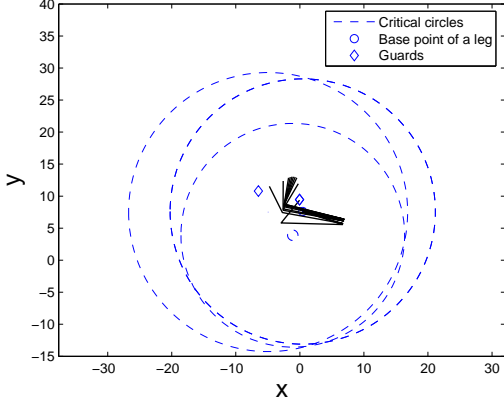


Fig. 20. Motion of leg 2: step 5.

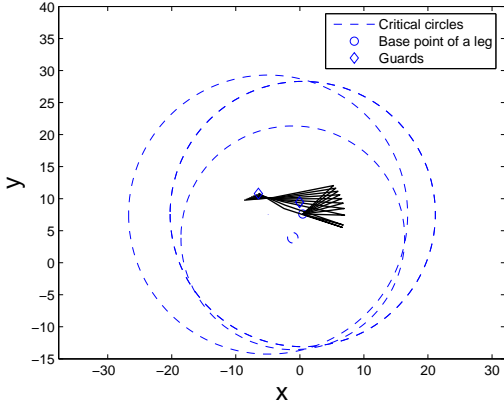


Fig. 21. Motion of leg 2: step 6.

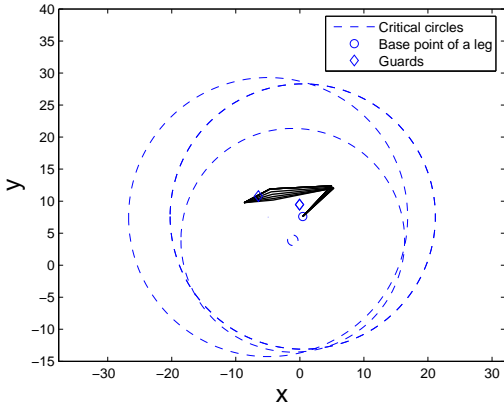


Fig. 22. Motion of leg 2: step 7.

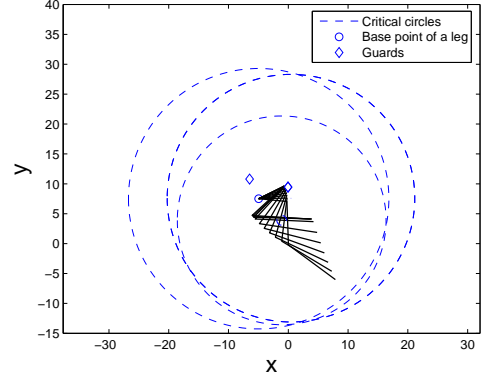


Fig. 23. Motion of leg 3: step 1.

Since  $\mathcal{C}$  is a fibration over  $W_A$ , a meaningful metric for  $\mathcal{C}$  is

$$ds^2 = a_1 dp^T dp + a_2 \sum_{j=1}^k du_j^T V_j^T V_j du_j, \quad a_1, a_2 > 0, \quad (7)$$

where  $a_1$  and  $a_2$  are two weights assigned to  $dp^T dp$  and  $\sum_{j=1}^k du_j^T V_j^T V_j du_j$ , respectively for they are quantities with different physical meaning. The column vectors of  $V_j \in \mathbb{R}^{n_j \times (n_j - 2)}$  forms a basis for the null space of the Jacobian  $J_j = \frac{\partial f_j}{\partial \Theta_j}$  of leg  $j$ , i.e.,

$$J_j V_j = 0.$$

$du_j$  denotes the incremental changes of the local coordinates on  $\tilde{\mathcal{C}}_j(p)$ .  $dp$  and  $V_j du_j$  stands for the infinitesimal motion along the base manifold and the fibre, respectively. The shortest path problem is to find a path  $(p(t), \Theta_1(t), \dots, \Theta_k(t))$  such that

$$\int_{t=0}^1 ds \quad (8)$$

is minimal. The optimal solution to (8) satisfies the geodesic equation

$$\ddot{v}_k + \Gamma_{ij}^k \dot{v}_i \dot{v}_j = 0 \quad (9)$$

where  $v = [p^T, u_1^T, \dots, u_k^T]^T$ , and  $\Gamma_{ij}^k$  denotes the Christoffel symbol of the metric (7). Solving (9) exactly is difficult. However, an approximation solution can be derived. Since a path from  $c_{\text{init}}$  to  $c_{\text{goal}}$  is globally optimal if and only if this path is also locally optimal, we construct an approximate shortest path in a way so that (i)  $p(t)$  connects  $p_{\text{init}}$  and  $p_{\text{goal}}$  and visits all  $p_i$ . Moreover,  $\int_{t=0}^1 \sqrt{dp^T dp}$  is minimal; (ii) There is minimal number of accordion moves, and each accordion move is minimal; (iii) Except for the accordion moves, there is no other motions along the fibre.

**Remark 2:** The path constructed in this way is shortest if no accordion moves are needed for we always achieve minimal  $ds = \sqrt{a_1 dp^T dp}$  infinitesimally, while it is only an approximation if there is at least one accordion move.

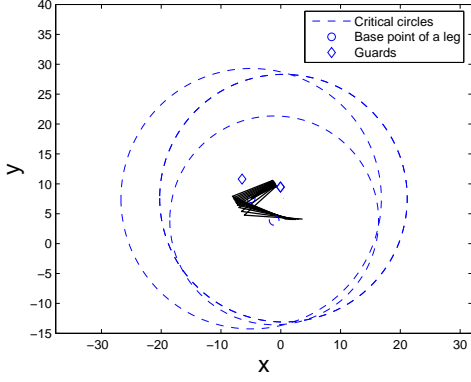


Fig. 24. Motion of leg 3: step 2.

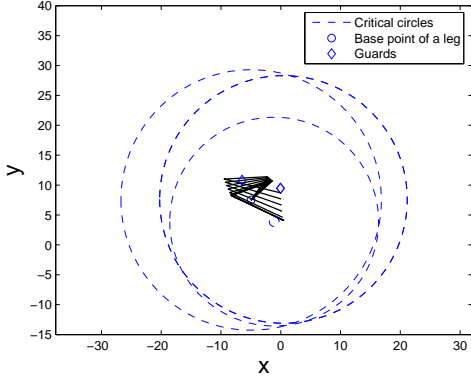


Fig. 25. Motion of leg 3: step 3.

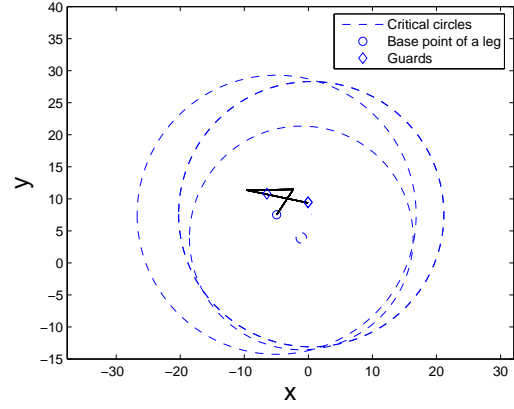


Fig. 26. Motion of leg 3: step 4.

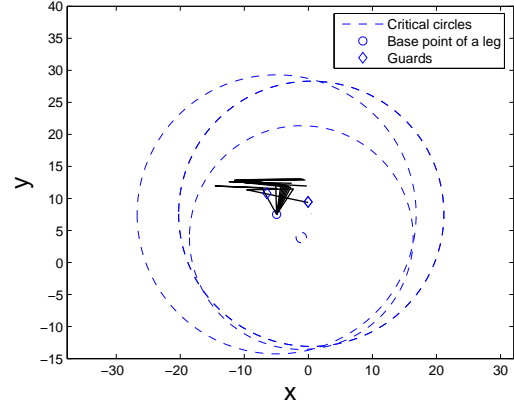


Fig. 27. Motion of leg 3: step 5.

(i) is generally a nonconvex and nonlinear optimization problem, since  $W_A$  could be nonconvex, and the objective function (the distance function) as well as the constraints are nonlinear. Mathematically, this problem can be described as

$$\begin{aligned} & \min \int_0^1 \|dp\| \\ & p(t) \in W_A, \forall t \in [0, 1] \\ & p_i \in \{p(t)\}, \forall i \\ & p_i \in \mathcal{A}_{\delta(i)} \end{aligned}$$

where  $\mathcal{A}_j, j \in J$  is the boundary arcs of the two-component cell of leg  $j$  that contains  $p_{\text{goal}}$ .  $\delta(J)$  is a permutation of  $J$  with  $\delta(J) = J$ . Solving this problem exactly is extremely hard, but a random search method (for example, the Controlled Random Search Method [34]) can be used to quickly find a good approximate solution. Using the minimal number of accordion moves has been solved in `ConstructPath`, and the minimal accordion move problem has been solved in [29]. Combining these two, (ii) is solved.

To solve (iii), we notice that for a local motion  $dp = [dx, dy]$  of the thorax endpoint,  $d\Theta_j^T d\Theta_j$  is minimized if and only if.

$$d\Theta_j = J_j^+ dp$$

where  $J_j^+ = J_j^T (J_j J_j^T)^{-1}$ .

Another important aspect about our planning algorithm is robustness. The sign-adjust move of leg  $j$  performed at a guard  $q_j$  is only feasible when  $\mathcal{C}_j(q_j)$  is connected. Since  $q_j \in \Sigma_j$

which is only 1-D, a small perturbation of the junction point in  $W_A$  (e.g., due to numerical errors) will violate the condition  $p \in \Sigma_j$ . When  $p$  moves into a two-component cell, then the sign-adjust move may fail. A remedy to this is to modify the path of the thorax in the neighborhood of  $q_j \in \Sigma_j$  so that a point  $q'_j$  in the interior of a one-component cell is reached. After the sign of leg  $j$  is adjusted to the desired one with  $p$  fixing at  $q'_j$ , we apply a constrained accordion move algorithm to ensure that the leg  $j$  stays in the right component of  $\mathcal{C}_j(p)$  just before its thorax endpoint enters the two-component cell containing  $p_{\text{goal}}$ . This resulting algorithm will also be robust to other errors such as the control and sensor errors if they are taken into account.

## VII. EXAMPLES

In this section, we demonstrate the correctness and complexity of our algorithm through two examples: a manipulator with three five-link legs (see Extension 1 for the video), and a manipulator with three five-link legs (see Extension 2 for the video). Movies of the motion plans are very helpful in understanding the figures.

In the first example, two of the three legs of the manipulator have three long links when  $A$  is fixed at  $p_{\text{goal}}$ . Figure 8 shows the manipulator in its starting and goal configurations. Our

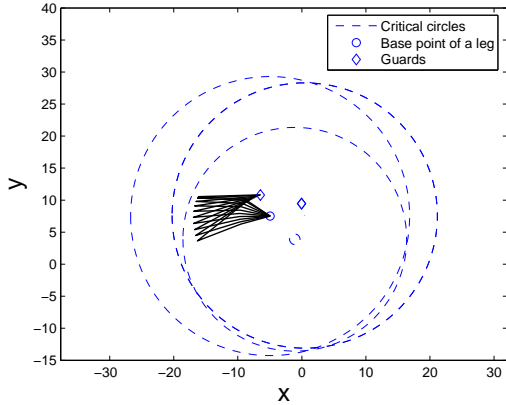


Fig. 28. Motion of leg 3: step 6.

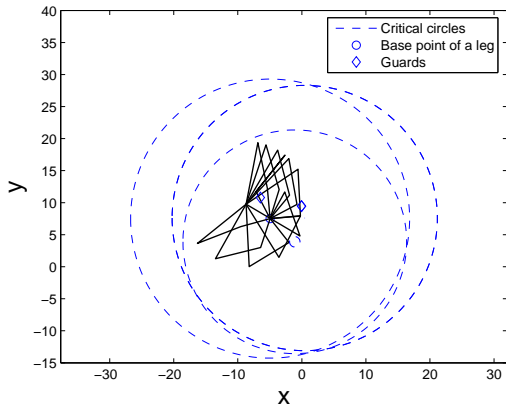


Fig. 29. Motion of leg 3: step 7.

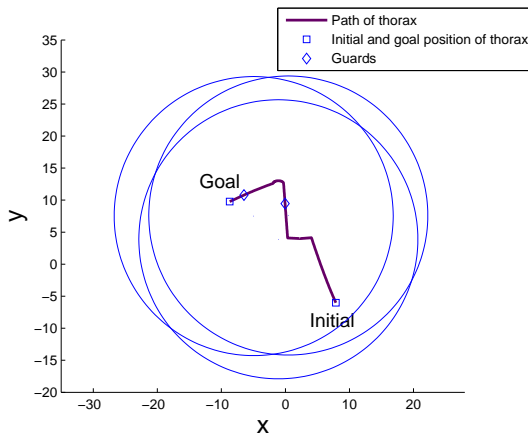


Fig. 30. Path of the thorax.

algorithm predicts  $J = \emptyset$ . Then the algorithm constructs a path in  $W_A$  from  $p_{\text{init}}$  to  $p_{\text{goal}}$ , drawn as the dark solid lines in Fig. 30. This path intersects the boundary of the two-component annular region of leg  $j$  that contains  $p_{\text{goal}}$  several times, among which  $q_j$ ,  $j = 1, 2$  are the last ones. These two points are the guards (drawn as diamonds) where sign-adjust moves are performed.

At  $q_j$ ,  $j = 1, 2$ , we check the sign of a pair of long links of leg  $j$  and see if it matches its sign at the goal. If not, we fix the other two legs and adjust the sign of the chosen long links in leg  $j$ . In this particular example, we chose the two longest links as the pair of long links, and we find that at  $q_1$  the sign of leg 1 does not match that at the goal (while at  $q_2$ , leg 2 has the same sign as the goal). Before leaving  $q_j$  via the next accordion move, the pair of long links of leg  $j$  was moved to the elbow-opposite configuration (recall that there are two configurations for these two links, one is “elbow up”, the other is “elbow down”), which has exactly the same sign as the goal configuration. The Trinkle-Milgram algorithm [29] is used to plan such a motion between the two elbow-opposite configurations. Figures 9 - 29 show the progress of the manipulation plan as the steps of the complete planning algorithm are carried out.

A bit more complex example in which the star-shaped manipulator has three five-link legs is shown in Extension 1. The computation time for path existence for star-shaped manipulators with less than 10 legs, and legs of less than 10 links is typically from less than 1 second to a few seconds when run in a Matlab, P4, WindowsXP system.

## VIII. DISCUSSION

Star-shaped manipulators are closed chain manipulators subject to multiple loop closure constraints. The C-space of these manipulators is often a lower-dimensional submanifold with high genus<sup>2</sup> embedded in the ambient space. Computing the silhouette of this manifold requires solving the extreme points of the manifold either in the ambient space whose dimension is much higher than that of the manifold itself, or in a set of local neighborhoods (local coordinate charts) whose number grows exponentially along with the genus of the submanifold. Although Canny’s algorithm is very efficient in general, there is difficulty in implementation for star-shaped manipulators. Second, the classical cylindrical decomposition of C-space (e.g. collin’s decomposition) is a partition into simple connected subsets of C-space called cells. However, this algorithm requires a description of the C-space in terms of a set of polynomials over its ambient space. Again because the dimension of the ambient space could be very high, the computation time of this algorithm could become formidable.

Our algorithm employs the special structural properties (fibration over the workspace) of the C-space of star-shaped manipulators. It avoids using the coordinates of the ambient space as well as the local coordinate charts that covers the C-space. In our algorithm the path existence and path construction are solved in polynomial time by combining the cell

<sup>2</sup>The genus of a surface is defined as the largest number of nonintersecting simple closed curves that can be drawn on the surface without separating it.

decomposition of the workspace (which is two dimensional and with simple shape) and the structure of the C-space of single-loop closed chains. The critical set  $\Sigma_j$ , which marks the change of the topology of the C-space of each leg, plays a key role in this algorithm.

## IX. CONCLUSION

In this paper, we studied the global structural properties of planar star-shaped manipulators. Via the analysis of the critical set  $\Sigma$ , we derived the global connectivity of the C-space, and necessary and sufficient conditions for path existence. Based on these results, we devised a complete polynomial algorithm for motion planning. Simulation examples were used to illustrate the key ideas behind the motion planning problem of planar star-shaped manipulators.

## APPENDIX: INDEX TO MULTIMEDIA EXTENSIONS

The multimedia extension page is found at <http://www.ijrr.org>.

**Table of Multimedia Extensions**

Extension	Type	Description
1	Video	A path planning simulation for three legged star-shaped manipulators having five links in each leg.
2	Video	A path planning simulation for three legged star-shaped manipulators having three links in each leg.

## ACKNOWLEDGMENT

The authors would like to thank Ryan Trinkle for help on the analysis of the solution existence algorithm, and the National Science Foundation for its support through grants 0139701 (DMS-FRG), 0413227 (IIS-RCV), and 0420703 (MRI).

## REFERENCES

- [1] M. Cherif and K.K. Gupta, *Planning Quasi-Static Fingertip Manipulation For Reconfiguring Objects*. IEEE Transactions on Robotics and Automation, Vol. 15, No. 5, PP. 837-848, 1999.
- [2] D. E. Koditschek, *Exact Robot Navigation by Means of Potential Functions: Some Topological Considerations*. IEEE International Conference on Robotics and Automation, PP. 1-6, 1987.
- [3] Lozano-Perez83, *Spatial Planning: A Configuration Space Approach*. IEEE Transactions on Computers, Vol. C-32, No. 2, PP. 108-119, 1983.
- [4] D.J. Jacobs, A.J. Reider, L.A. Kuhn, and M.F. Thorpe, *Protein Flexibility Predictions Using Graph Theory*. PROTEINS: Structure, Function, and Genetics, 44:150-165.
- [5] J. Cortés, T. Siméon, and J.P. Laumond, *A Random Loop Generator for Planning the Motions of Closed Kinematic Chains using PRM Methods*. In Proceedings of the 2002 IEEE International Conference on Robotics and Automation, pages 2141-2146, 2002.
- [6] J. Cortes and T. Siméon, *Probabilistic Motion Planning for Parallel Mechanisms*. In Proceedings of the 2003 IEEE International Conference on Robotics and Automation, pages 4354-4359, 2003.
- [7] E. Rimon and D. E. Koditschek, *Exact Robot Navigation Using Cost Functions: The Case of Distinct Spherical Boundaries in  $E^n$* . IEEE International Conference on Robotics and Automation, PP. 1791-1796, 1988.
- [8] D. Hsu, J.C. Latombe, and R. Motwani, *Path Planning in Expansive Configuration Spaces*. IEEE International Conference on Robotics and Automation, 1997.
- [9] E. Rimon and D. E. Koditschek, *The Construction of Analytic Diffeomorphisms for Exact Robot Navigation on Star Worlds*. IEEE International Conference on Robotics and Automation, PP. 21-26, 1989.
- [10] N. Shvalb, M. Shoham, D. Blanc *The Configuration Space of an Arachnoid Mechanism*. To appear in Forum Mathematicum 2005.
- [11] J.-C. Hausmann and A. Knutson, *The cohomology ring of polygon spaces*. Ann. Inst. Fourier, Vol. 48, PP. 281-321, 1998.
- [12] Y. Kamiyama, M. Tezuka, and T. Toma, *Homology of the Configuration Spaces of Quasi-Equilateral Polygon Linkages*. Transactions of the American Mathematical Society, Vol. 350, No. 12, PP. 4869-4896, 1998.
- [13] J. Barraquand and J.-C. Latombe, *Nonholonomic Multibody Mobile Robots: Controllability and motion planning in the presence of obstacles*. IEEE International Conference on Robotics and Automation, PP. 2328-2335, 1991.
- [14] J.W. Burdick. On the inverse kinematics of redundant manipulators: characterization of the self-motion manifolds. *IEEE Int. Conf. on Robotics and Automation (ICRA)*, pages 264–270, May 1989.
- [15] J. Schwartz, J. Hopcroft, and M. Sharir, *Planning, Geometry, and Complexity of Robot Motion*. Ablex, 1987.
- [16] S. M. LaValle and J. J. Kuffner, *Rapidly-exploring random trees: Progress and prospects*. In B. R. Donald, K. M. Lynch, and D. Rus, editors, *Algorithmic and Computational Robotics: New Directions*, pages 293-308, A K Peters, Wellesley, MA, 2001.
- [17] J.T. Schwartz and M. Sharir, *On the piano movers II. General techniques for computing topological properties on real algebraic manifolds*. Adv. Appl. Math., vol.4, PP. 298-351, 1983.
- [18] L. Han and N.M. Amato, *A kinematics-based probabilistic roadmap method for closed chain systems*. in *Algorithmic and Computational Robotics: New Directions*, B.R. Donald, K.M. Lynch, and D. Rus, Eds. AK Peters, Wellesley, PP. 233-246, 2001.
- [19] N. Amato, B. Bayazit, L. Dale, C. Jones, and D. Vallejo, *OBPRM: An obstacle-based PRM for 3d workspaces*. in *Robotics: The Algorithmic Perspective*, P. Agarwal, L. Kavraki, and M. Mason, Eds. Natick, MA: A.K. Peters, 1998, PP. 156-168.
- [20] V. Boor, M. Overmars, and A.F. van der Stappen, *The Gaussian sampling strategy for probabilistic roadmap planners*. IEEE International Conference on Robotics and Automation, 1999.
- [21] R. Bohlin and L. Kavraki, *Path planning using lazy PRM*. IEEE International Conference on Robotics and Automation, PP. 521-528, 2000.
- [22] J.J. Kuffner and S.M. LaValle, *RRT-Connect: An Efficient Approach to Single-Query Path Planning*. IEEE International Conference on Robotics and Automation, PP. 995-1001, 2000.
- [23] S.M. LaValle and J.J. Kuffner, *Randomized kinodynamic planning*. IEEE International Conference on Robotics and Automation, 1999.
- [24] J.F. Canny, *The Complexity of Robot Motion Planning*. Cambridge, MA: MIT Press, 1988.
- [25] M. Kapovich and J. Millson, *On the moduli spaces of polygons in the Euclidean plane*. Journal of Differential Geometry, Vol. 42, PP. 133-164, 1995.
- [26] L.E. Kavraki, P. Švestka, J.C. Latombe, and M.H. Overmars, *Probabilistic Roadmaps for path planning in high-dimensional configuration space*. IEEE Transactions on Robotics and Automation, 12(4):566-580, 1996.
- [27] J.C. Latombe, *Robot Motion PLanning*. Kluwer Academic Publishers, 1992.
- [28] R.J. Milgram and J.C. Trinkle, *The Geometry of Configuration Spaces for Closed Chains in Two and Three Dimensions*. Homology Homotopy and Applications, 6(1):237-267, 2004.
- [29] J.C. Trinkle and R.J. Milgram, *Complete Path Planning for Closed Kinematic Chains with Spherical Joints*. International Journal of Robotics Research, 21(9):773-789, December, 2002.
- [30] J. Yakey, S. M. LaValle, and L. E. Kavraki, *Randomized path planning for linkages with closed kinematic chains*. IEEE Transactions on Robotics and Automation, 17(6):951–958, December 2001.
- [31] J. Sefrioui and C.M. Gosselin, *On the quadratic nature of the singularity curves of planar three-degree-of-freedom parallel manipulators*. Mechanism and Machine Theory, 30(4):533–551, May 1995.
- [32] A.K. Dash, C. I-Ming, Y. Song-Huat and Y. Guilin, *Singularity-free path planning of parallel manipulators using clustering algorithm and line geometry*. Robotics and Automation, 1:761- 766, September 2003.
- [33] D.N. Nenchev, Y. Tsumaki and M. Uchiyama *Singularity-Consistent Parameterization of Robot Motion and Control* The International Journal of Robotics Research, 19(2):159-182, 2000.
- [34] J.R. Banga and W.D. Seider, *Global Optimization of Chemical Processes Using Stochastic Algorithms*, State of the Art in Global Optimization:

Computational Methods and Applications, C.A. Floudas and P.M. Pardalos (Eds.), Kluwer Academic Publishers, pages 563-583, 1996.